

Case History

Mapping of apparent magnetic susceptibility and the identification of fractures: A case study from the Eye-Dashwa Lakes pluton, Atikokan, Ontario

Madeline D. Lee¹, William A. Morris¹, and Hernan A. Ugalde¹

ABSTRACT

In situ magnetic-susceptibility measurements are only possible on outcrops, which are often limited by overburden and water bodies. An alternative approach is to derive an apparent susceptibility map from total-magnetic-intensity (TMI) surveys, which was done in this study for the Eye-Dashwa Lakes pluton near Atikokan, Ontario. Susceptibility logs of cores directly link alteration to systematic changes in the amount and composition of magnetic minerals. The surficial distribution of alteration zones was originally estimated from a limited number of in situ magnetic-susceptibility measurements. Here, through forward modeling of the TMI data set, susceptibility data are used to validate the apparent susceptibility data set. The modeling accounts for the bathymetric surface of all lakes that cover the area. A two-step process of bulk and local-scale modeling was used to estimate apparent susceptibility patterns. Bulk magnetic susceptibility is used as an indicator of overall alteration content, and local-scale apparent magnetic-susceptibility values are computed using a forward-modeling routine. The new apparent magnetic data set indicates northwest and northeast linears, which are the same as those seen in previous studies.

INTRODUCTION

Magnetic anomalies are created through the juxtaposition of rock masses with contrasting physical properties in the presence of a constant applied magnetic field (the present earth's magnetic field). These physical-property contrasts are related to changes in the mag-

netic susceptibility, and/or the presence of natural remanent magnetization (NRM) in the rock units being sampled. Magnetic susceptibility is primarily a function of magnetite content, in addition to titanium content, oxidation state, and mineral grain size (Harding et al., 1988). As such, magnetic susceptibility often is used in characterization studies of rock lithology and alteration. A magnetic-susceptibility survey requires significant rock exposure to obtain proper coverage. Unfortunately, it is common to have a limited number of outcrops, or much of the region may be covered by lakes and overburden. Even when outcrop is more extensive, there are limitations to an in situ field-mapping program. Often magnetic susceptibility can be only coarsely sampled at intervals on the order of tens to hundreds of meters, and as such, can preclude the resolution of local-scale geologic features. On the other hand, both ground and airborne total-magnetic-intensity (TMI) surveys can provide more detailed information because of their higher sampling rate. With this notion, an alternative approach to in situ magnetic-susceptibility surveying is to derive an apparent magnetic susceptibility from the TMI data.

Various studies have been carried out to map the Eye-Dashwa pluton and determine its suitability as a potential site for underground disposal of nuclear fuel waste (Brown et al., 1980; Stone, 1980; Dugal et al., 1981; Hillary, 1982; Brown et al., 1984; Morris Magnetism [personal communication], 1985; Lapointe et al., 1986; Harding et al., 1988). Central to the selection of an area for an underground disposal facility is that the geology be as structurally homogeneous as possible. More specifically, it is recognized that the existence of fractures and faults invariably will affect stability of the containment and enable subsurface water movement (Kamineni and Stone, 1983). In the past, initial analysis of fracture and fault configurations of the pluton was accomplished using a number of geotechnical methods that were able to map faults and fractures both directly and indirectly — including aerial photography, magnetic surveys, air-

Manuscript received by the Editor 24 February 2009; revised manuscript received 2 December 2009; published online 9 June 2010.

¹McMaster University, School of Geography and Earth Sciences, Hamilton, Ontario, Canada. E-mail: leemd@mcmaster.ca; morriswa@mcmaster.ca; ugaldeh@mcmaster.ca.

© 2010 Society of Exploration Geophysicists. All rights reserved.

borne VLF-EM, and ground geologic mapping (Brown et al., 1984). Indirect methods were commonly used because the Eye-Dashwa Lakes pluton mainly has between 5% and less outcrop, based on aerial photograph analyses (Brown et al., 1984). On a regional scale, distribution of fracture systems is commonly inferred from identification of lineaments on images of the topography or aerial photography (Figure 1a). Although these methods can outline large-scale structures, they are incapable of detecting the degree of alteration associated with fluid flow in a fracture.

In this article, we apply an alternative apparent magnetic-susceptibility method to a ground magnetic data set from the Eye-Dashwa Lakes pluton, in northern Ontario, Canada. We perform magnetic mapping, using both ground TMI and in situ magnetic-susceptibility sampling. This method works because porous rock and fractures are associated directly with systematic alteration of iron-titanium oxides (FeTiO_3) that with increasing oxidation, exhibit a progressive reduction in magnetite grain size followed by alteration to hematite (Lapointe et al., 1986; Harding et al., 1988). Both processes yield a

reduction in magnetic susceptibility and, therefore, a reduced TMI anomaly. Because both ground TMI and magnetic-susceptibility surveys were conducted over the same area, this provides an ideal case study to test the veracity of apparent magnetic-susceptibility data computed from a TMI data set. Validity of the apparent susceptibility distribution is tested through comparison with in situ observed susceptibility measurements using both visual and statistical methodologies.

Additionally, a drilling and core-logging project was conducted within the east-southeast corner of the pluton to assess rock homogeneity for a future waste-repository site. Five boreholes (ATK-1 through ATK-5) were drilled less than 1 km from the area reported in this study. Dugal et al. (1981) show that the rock type changed very little at the Atikokan drilling location. Furthermore, variation of modal mineral percentages with depth in the boreholes was minimal. Detailed magnetic-susceptibility measurements performed on cores from each of the five boreholes permitted subdivision of the granite into different alteration levels. Subsequent magnetic coercivity and

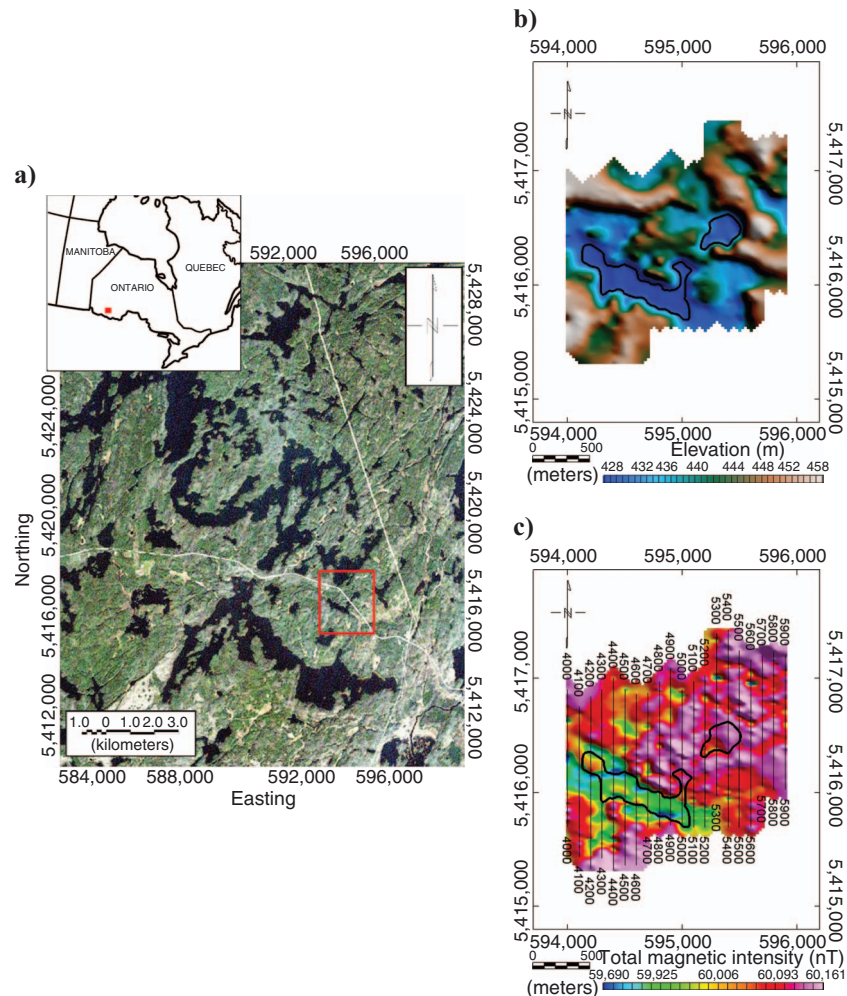


Figure 1. (a) Aerial photograph of the Eye-Dashwa Lakes pluton area. The primary regional scale trend is visible (northwest-southeast) along with a secondary orthogonal trend (northeast-southwest). The red box indicates the study site. (b) Diurnally corrected and leveled-ground total-magnetic-intensity data set with survey-line layout. The TMI data set was terrain-corrected for the source-sensor distance (2 m); however, the effects were negligible. (c) Known topography of the study site derived from the TMI survey.

petrologic studies of polished thin sections indicated that the varying alteration levels corresponded to the progressive alteration of primary igneous magnetite to secondary hematite (Kamineni and Dugal, 1981, 1982; Hillary et al., 1985; Lapointe et al., 1986). Detailed magnetic-susceptibility measurements from this core study provide the control parameters by which we have assessed our derived apparent susceptibility models. It is important to note that reference susceptibility values provided by the core study represent a rock average based on thousands of individual measurements.

GEOLOGY

The Eye-Dashwa Lakes pluton is 15-km north-northeast of Atikokan, Ontario and is part of the Superior Province of the Canadian Shield. The pluton is of Kenoran age (2.5 Ga) and is a massive elliptical medium-to-coarse-grained biotite-hornblende granite (Brown, 1980; Stone and Kamineni, 1982; Kamineni and Stone, 1983; Lapointe et al., 1986). The Dashwa gneiss, into which the pluton intrudes, is a tonalitic to amphibolitic gneiss complex (Brown et al., 1980). The gneiss exhibits a complex metamorphic and tectonic history that is not replicated within the pluton, indicating that the pluton was emplaced post-tectonically. Furthermore, the gneiss is shown to have a higher density of lineaments (fractures) than the granite. However, there are no obvious displacements of the contact between the pluton and the gneiss, suggesting that this area has not been subjected to extensive faulting since emplacement of the granite mass. Fractures within the pluton are infilled with a variety of minerals including chlorite, calcite, clay, gypsum, epidote, quartz, and muscovite (Brown et al., 1980). Different proportions and combinations of these minerals provide insight into the fluids that have passed through the fractures with time. Typically, early, high-temperature fracture systems that formed during the initial cooling of the pluton are epidote-rich (2.6 Ga to 2.4 Ga), and recent remobilization and rejuvenation of existing fractures are marked by the presence of low-temperature hematite (Kamineni and Stone, 1983). Typically epidote, chlorite, or hematite is the dominant infill material (Brown et al., 1980). Because these minerals have significant iron content and are known to have differing specific magnetic-susceptibility values, their presence in a homogeneous granite can be tied to magnetic-anomaly variations.

METHODOLOGY AND RESULTS

Bathymetry estimation

The magnetic field intensity at any point above the earth's surface is, in part, defined by the source-sensor distance. During a ground magnetic survey, the sensor is held at a near-constant height above the local topographic surface. In this study area, there are a number of lakes. Because the TMI survey was completed during the winter, measurements over the lakes were made from the ice surface, resulting in an increased source-sensor distance for all the lake-based measurements. Because of the remote location of the study site, there is no readily available source of bathymetric data for the lakes. Accordingly, the initial geophysical anomaly maps reported for the Atikokan study area did not include any consideration of the possi-

ble effect of the bathymetry on the observed TMI signal. To correct the magnetic data for this, bathymetry is required. Therefore, we tried two approaches to estimate bathymetry.

The first is based on the assumption that shoreline topography around each margin of a lake has some relationship to the morphology of the water-rock interface under the lake. Assuming there are no sharp discontinuities between outcrops on either side of the lake, the bathymetry along each cut line can be estimated by interpolating the topography measured on the shores using a low-order polynomial (B-spline). Clearly there will be limitations to calculating a valid bathymetry through this method. First, like any other polynomial line-fitting approach in a situation with limited data input, it is quite possible to introduce dramatic overshoots that have no real significance. For example, if the tension of the polynomial is too low, then unrealistic bathymetry values that place the lake floor far deeper than what would be expected are produced. Secondly, the bathymetry determined by the polynomial fit will be strongly influenced by the topographic gradient at the lake edges. If a steep gradient exists at the lake edge, this will result in a bathymetry deeper than what is likely the true depth. The contrary would hold true as well, resulting in values that are too shallow. Finally, any discontinuities (faults) in the middle of the lake will not be resolved by this method. However, an assessment of the regional geology and observed ground magnetic data allows one to determine whether there are any faults beneath the lake, and therefore, whether the method is valid.

Figure 1b shows the diurnally corrected and leveled ground magnetic data. The TMI survey was conducted in two parts; first in January of 1985 and then in March of 1985 by Morris Magnetics, Inc. Twenty-one north-south survey lines were conducted with a line spacing of 100 m. A constant sample spacing of 10 m was used in the study area for a total of 3700 samples. An EDA PPM-500 was used, which was capable of measuring both total field intensity and vertical gradient. An EDA PPM-400 was used as a base station from which all diurnal variations were recorded. Although all diurnal variations throughout the TMI survey were quite low, they were still corrected for using a linear interpolation algorithm. Because the survey was conducted over two time periods, the data was normalized through common observations in the two surveys. According to TMI data and topographic data (Figure 1c), there are visible northwest and northeast lineaments in the study area. Furthermore, although the lake appears to be coincident with the magnetic anomaly low (green), the trend of the shoreline (west-northwest to east-southeast) is different from that of the anomaly (northwest-southeast). This suggests the magnetic low is caused by a geologic feature rather than the lake.

Figure 2a shows results of the application of the spline-based approach for bathymetry estimation on profile 4400, through the center of the large lake (see Figure 1b for location). For explanation purposes, one moderate tension of 0.3 and two extreme interpolation cases are given, where no tension (0) and high tension (0.5) were considered on the B-spline algorithm, leading to overly deep and shallow bathymetry estimations, respectively.

The second approach to bathymetry mapping was based on simple 2.5D forward magnetic-anomaly models of the lake geometry. For this model, the water of the lake is assigned a magnetic-susceptibility value of zero and we assume there are no changes in susceptibility of the granite below the lake bottom. For this to be true, we consider only the longer-wavelength components of the observed

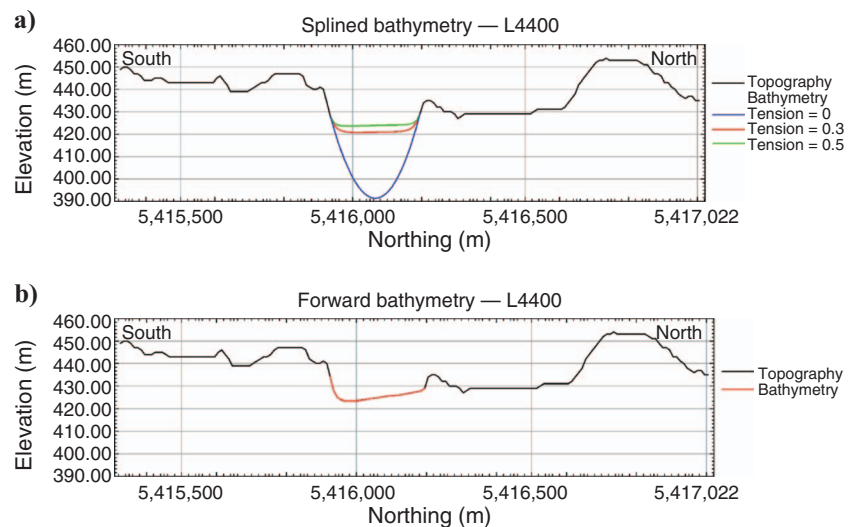
TMI profiles (features greater than 100 m) to represent bathymetry, as magnetic-susceptibility variations in the granite will introduce short-wavelength anomalies (features between 50 m and 100 m). Under the above assumptions, the only remaining variable that affects the calculated magnetic field is the depth of the water (function of source-sensor separation). As input information, we know the x , y , z location of each TMI measurement. Hence, computing the optimum model match between the observed and computed magnetic field provides an estimate of the bathymetry along each cutline. If the observed magnetic anomaly were purely a consequence of increased source-sensor separation over the lake, then the underlying rock slab should be treated as an unaltered, massive, homogeneous rock unit, which previous drill-core studies indicate has a constant magnetic susceptibility of 0.0175 SI (Table 1). Figure 2b shows the estimated bathymetry derived by forward modeling of the TMI over the same line used in Figure 2a. Based on the close similarity between results derived from forward modeling and the B-spline approach using a tension of 0.3 for line L4400, an interpolated depth for each lake was calculated using the same 0.3 tension. Both the interpolated and forward-modeled bathymetry estimates then were gridded at a 50-m cell size using a minimum curvature algorithm. These methods produced similar bathymetry results, although there are minor differences. Figure 3 shows a comparison between the interpolated and forward-modeled bathymetry grids. The average difference between the two methods was 0.65 ± 3.67 m (Figure 3c), which represents 4.33% of the maximum depths for the two lakes found in the study area (15 m).

Given the similar results obtained with both methods, the interpolated bathymetric surface was used as reference for correcting magnetic data for the variations in source-sensor separation. Because the process involves converting profile data from a nonflat plane to another nonflat plane parallel to the combined topographic and bathymetric surface, we used a second-order Taylor series approximation (Pilkington and Thurston, 2001). This correction was 14.1 ± 2.1 nT in deeper parts of the lakes (15 m), or 0.7% of the dynamic range of the data before the correction (59450 to 60550 nT). Although not a major correction, this process ensures that observed anomalies are of lithologic origin and not due to source-sensor separation variations.

Magnetic susceptibility

The original magnetic-susceptibility survey was conducted in October 1984 by Morris Magnetics, Inc. (Morris Magnetics, personal communication, 1985). All survey lines ran north-south with a line separation of 100 m, exactly over the same lines used for the ground magnetic survey (Figure 1b), but with a broader spacing along the lines. In areas of outcrop, the sample spacing was 100 m with a total of 343 samples collected in the total study area. Readings were conducted using a Sapphire Instruments susceptibility bridge. Six measurements were taken at each site and then mean and standard deviation were calculated for each site. The mean provides insight into the oxide mineralogy of each site and the standard deviation gives a measure of the homogeneity of each site. Although direct suscepti-

Figure 2. Cross section along profile L4400. (a) Bathymetry results from the application of a B-spline interpolator. Accepted bathymetry is shown (tension = 0.3) in green along with known topography (black) and the bathymetry results from the application of high tension (red) and no tension (blue). (b) Forward-modeled bathymetry results (red) along with known topography (black).



bility measurements still can be gridded to provide a general view of alteration patterns, the limited sampled spacing precludes their use for finer detailed mapping. Therefore, we use forward modeling of the bathymetry-corrected ground TMI data.

There are a number of ways to approach this problem. Each involves analyses at two distinct levels of spatial resolution — the regional and local scales.

Apparent bulk magnetic susceptibility

Prior to any sort of fracture mapping, a calculation of bulk (regional) magnetic susceptibility for the entire study area should be found. This will indicate the level of alteration occurring within the granite. Taking a regional-scale approach, if the Eye-Dashwa Lakes pluton granite is indeed truly homogeneous, then the optimum match between the observed and calculated TMI for a 3D slab of the entire study area should have the magnetic susceptibility associated with nonfractured, unaltered granite. Furthermore, any difference between individual observed and computed TMI values should have an average value of zero and a variance that reflects the presence of noise in the original observation data. On the other hand, depending on the extent and spatial distribution of fracture-related TMI reduction, and if there has been any significant regional alteration of the slab, then the estimated bulk magnetic susceptibility will be systematically lower. Localized alteration, associated with fracture systems, should produce localized reductions in the TMI signal.

The 3D geometry of the slab is constrained by the combined interpolated bathymetric and topographic surfaces on top and a lower flat surface located below the minimum of the topography-bathymetry surface at bottom. The horizontal extension is unlimited to avoid

edge effects. Using an ambient field (IGRF 1985) of 60175 nT with an inclination and declination of 77° and 0.4° E, respectively, magnetic susceptibility of the generated granite slab is varied. The rms error associated with each TMI data set produced by the synthetic rock slab of various magnetic susceptibilities (0.001, 0.0125, 0.015, 0.0175, and 0.02 SI) was calculated in both profile and grid format:

$$\text{rms error} = \sqrt{\frac{\sum_{i=1}^n (x_{1,i} - x_{2,i})^2}{n}}, \tag{1}$$

where $x_{1,i}$ is the point x,y in the observed data set and $x_{2,i}$ is the point x,y in the synthetic data set with identical coordinates. In most cases, an rms error of 0 is unattainable due to local scale variations (mineralogy, topography, overburden thickness) within the original data set that cannot be resolved in the synthetically derived data set. As can be seen in Figure 4, no rms error less than 98.18 was achieved, which corresponds to a magnetic susceptibility of 0.0125 SI. As discussed above, the value of homogeneous granite within the study area is 0.0175 SI. Therefore, this shows a reduction in magnetic mineral content occurring within the rock caused by alteration. Figure 5a shows the magnetic intensity distribution produced by a 3D slab with a susceptibility of 0.0125 SI. To see the spatial distribution differences between the observed magnetic intensity and synthetically derived magnetic intensity, a difference grid was produced in Figure 5b.

Apparent local magnetic susceptibility

To derive more detail (local scale) on the spatial fluctuations of susceptibility, we derived apparent susceptibility by computing 2.5D forward models for each of the original ground TMI profiles. Knowing the morphology of the bedrock surface, the TMI, and the

local earth’s magnetic field parameters, the only variable remaining is local susceptibility distribution. In these models, no magnetic remanence was taken into consideration in agreement with the results derived from previous rock-property measurements (Lapointe et al., 1986; Harding et al., 1988). Once again, an ambient field of 60,175 nT with an inclination and declination of 77° and 0.4° E, respectively, is used. Individual alteration zones were geometrically defined as simple dipping slabs having a susceptibility that is distinct from the regional susceptibility, which was used to estimate the background signal. All the alteration zones are subvertically (80° to 90°) dipping to the north, which was the dominant dip direction indicated by Brown et al. (1980), Stone (1980), Dugal et al. (1981), Hillary (1982), and Morris Magnetics (personal communication, 1985). Figure 6 shows one of the 2.5D models along line L4400, which is the same profile as Figure 2. The depth extent of the alteration zones represented by the slabs was kept at a uniform 150 m because we are interested only in modeling short-wavelength anomalies, and geologic features greater than this depth would not produce any significant high-frequency magnetic anomalies. Just as with the regional-scale

Table 1. Influence of fracture-filling materials and their characteristics on the mean magnetic susceptibility of granite (after Hillary et al., 1985). The value presented for unaltered granite is an average of the range provided by Kamineni and Dugal (1981, 1982).

Fracture-zone type	Fracture-filling materials	Mean magnetic susceptibility (SI)
Moderate to subhorizontal dip	Epidote alone	0.0111
	Epidote (+ minor chlorite)	0.0076
	Chlorite (+ minor epidote)	0.0062
	Chlorite (without epidote)	0.0054
Steep to subvertical dip	Epidote alone	0.0103
	Epidote (+ minor chlorite)	0.0066
	Chlorite (+ minor epidote)	0.0038
	Chlorite (without epidote)	0.0034
Any dip	Any filling of clay or geothite	0.0035
Nonfractured; unaltered granite		0.0175

apparent susceptibility calculation, increasing the depth extent of the source body would result in a systematically lower value for the susceptibility, thus the obtained values are maximum bounds for the local magnetic susceptibility.

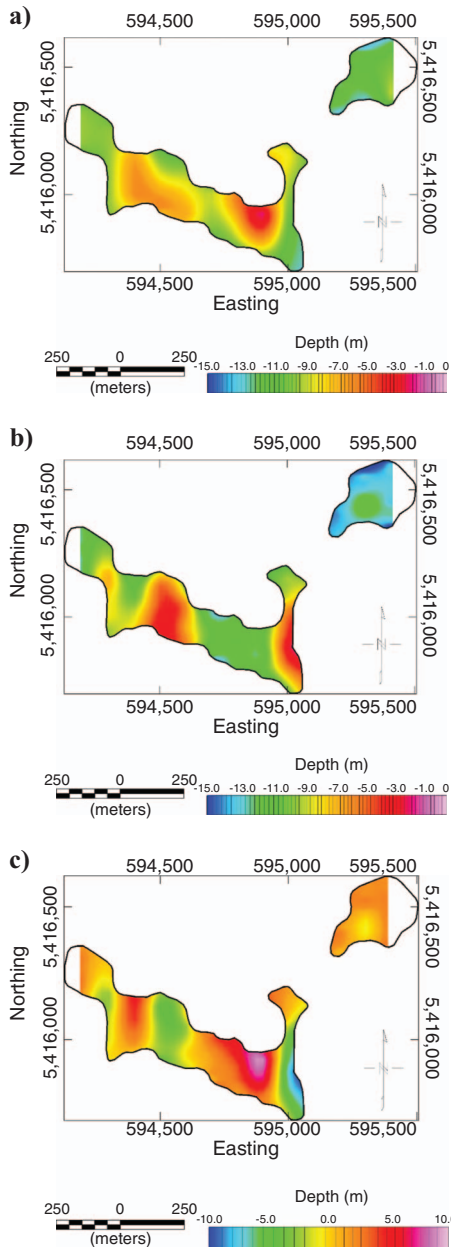


Figure 3. Grid comparison of (a) interpolated and (b) forward-modeled bathymetries. Both data sets have been gridded using a minimum-curvature interpolation scheme with identical-color table ranges. Observation points are marked +. (c) The calculated difference between the two bathymetry data sets also is gridded using a minimum-curvature routine. The most notable difference between the two bathymetries is the geographic location of the depth maximums, which are highlighted in the difference grid (blue and pink).

Two other constraints were applied to the local-scale modeling approach. First, ground magnetic surveys are notoriously noisy, especially when looking at low-amplitude magnetic anomalies. To address this issue, we applied a Naudy nonlinear low-pass filter (cutoff wavelength of 50 m) to the original TMI profile data and desampled the data to an observation point every 20 m. Secondly, it is incorrect to tie the presence of an alteration zone to a single observation point because there is no degree of confidence in this observation. Hence the width of all modeled slabs (alteration zones) is set at a minimum of three observation points, which corresponds to a minimum slab thickness of 40 m.

Magnetic-susceptibility values derived from the 2.5D cross sections are gridded to show their distribution over the entire survey area. Although this is changing from 2.5D (elongate prism) to 3D (grid) source interpretation, a certain level of assumption needs to be applied that all sources are considered 2.5D. In this case, the apparent magnetic susceptibility is validated relative to the observed magnetic susceptibility, which of necessity must be done on a topographic surface. Although, this does not provide a full, precise view of the 3D perspective of the apparent magnetic susceptibility, the results prove to be geologically reasonable as well as simple and straightforward. The apparent magnetic-susceptibility distribution derived from the 2.5D forward models displayed as a map exhibits large- and small-scale subparallel northwest trends (Figure 7a). The observed magnetic susceptibility (Figure 7b) exhibits similar trends, both in direction and scale. This dominant lineament direction of northwest agrees with the fracture populations discussed in Brown et al. (1980), Stone (1980), Dugal et al. (1981), Hillary (1982), and Morris (1985). It is to be noted that a prominent DC shift exists between the two data sets, where the apparent magnetic susceptibility has an overall higher range of values. To quantify this DC shift, both grids are made to have near-identical dynamic ranges in color (2.8×10^{-2} SI) but not the same origin (Figure 7). This results in a difference of 0.8×10^{-2} SI and is addressed further in the discussion section.

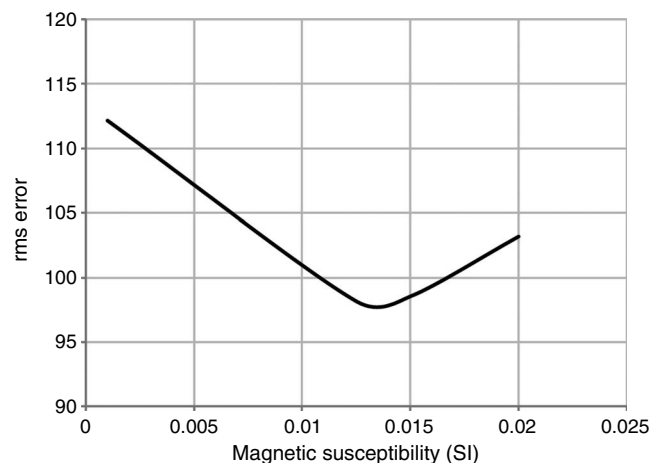


Figure 4. Root-mean-square error versus magnetic susceptibility of synthetic rock slab. The rms error is calculated from the difference between observed TMI and TMI derived from various magnetic-susceptibility values of the synthetic 3D rock slab. The lowest rms error achieved is 98.18 for a magnetic susceptibility of 0.0125 SI. This indicates regional reduction in magnetic content of the study area.

DISCUSSION

The two bathymetry estimation methods yielded similar results. Yet it was important that the magnetic susceptibility of the rocks under the lake remained constant. Therefore, any observed TMI lows were accommodated through a calculated deeper bathymetry in the forward-modeling process. However, if a portion of the lake actually is underlain by a sufficiently large (compared to the survey resolution) fracture, then the observed TMI signal at that point will be lower as a consequence of the reduced susceptibility level. Thus, forward-

modeled bathymetric lows represent alteration zones. By calculating the summary grid that represents the difference between the interpolated and forward-modeled bathymetry estimates, negative differences might suggest the presence of underlying altered fractures. When comparing the areas of bathymetry differences on the lakes (green and blue zones on Figure 2c) with the minimum susceptibility zones estimated by forward modeling (Figure 7a), they correspond closely. Thus, in this particular case of homogeneous lithologies, the two methods for bathymetry estimation also are able to map alteration zones beneath the lakes.

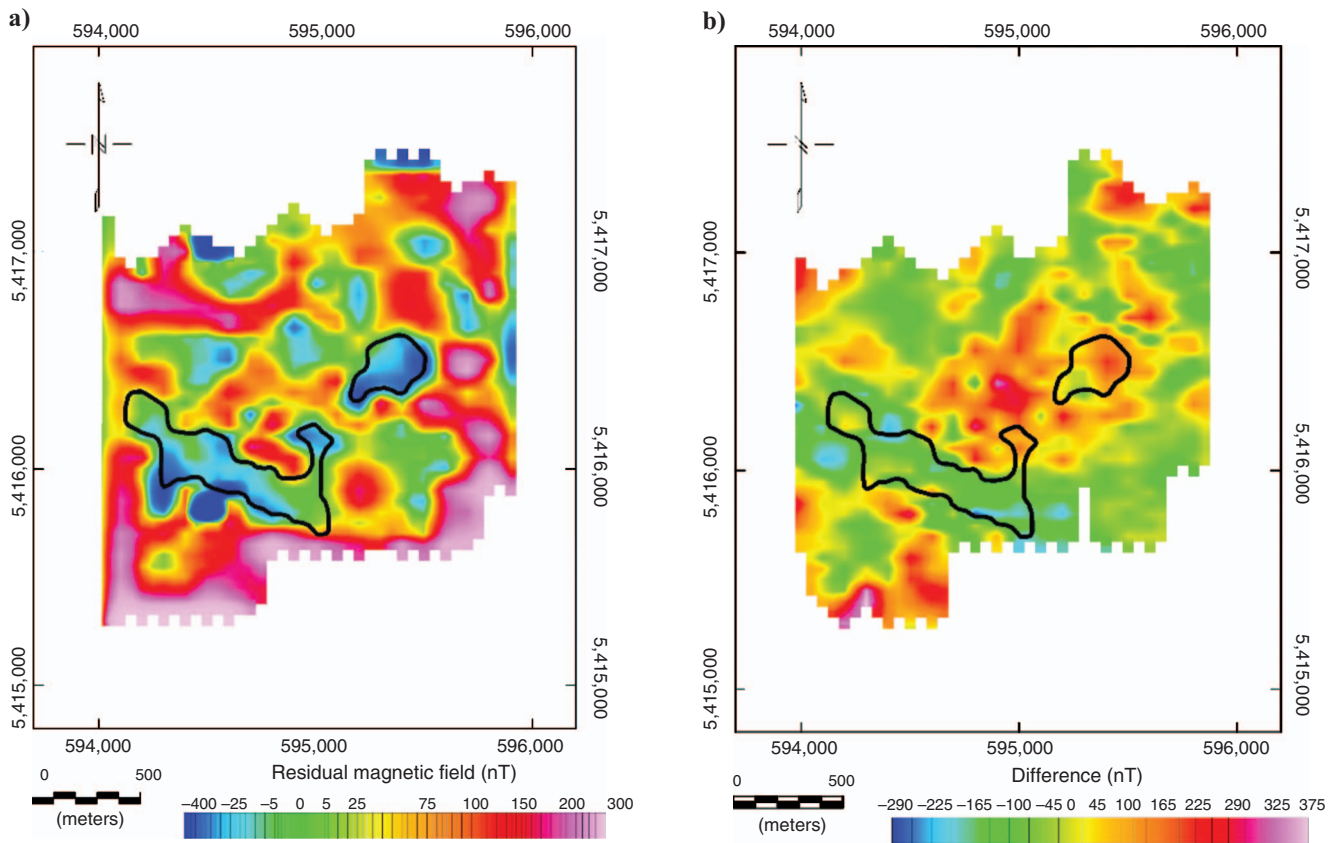


Figure 5. (a) Residual magnetic field of a synthetic 3D rock slab with a magnetic susceptibility of 0.0125 SI. (b) The difference between the observed residual magnetic field and the synthetic residual magnetic field produced by a rock slab with a magnetic susceptibility of 0.0125 SI.

Downloaded 10/28/14 to 173.206.187.50. Redistribution subject to SEG license or copyright; see Terms of Use at http://library.seg.org/

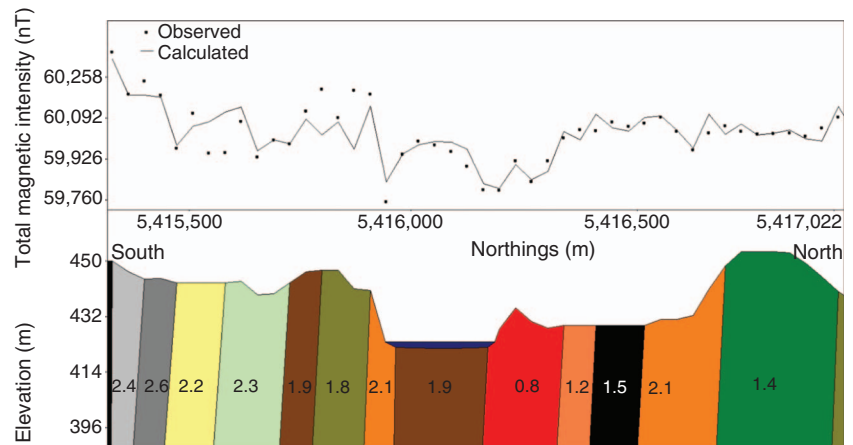
In terms of the estimated apparent magnetic susceptibilities, a qualitative assessment is deemed insufficient. Therefore, a numerical approach is taken to assess how similar the apparent magnetic susceptibility is to the observed magnetic susceptibility. This involves generating log-percent frequency histograms of both magnetic-susceptibility data sets (Figure 8). Visually, both the apparent susceptibility and observed susceptibility display a bimodal normal distribution. Taking this one step further, displaying both data sets as cumulative frequency-probability plots once again shows two populations in the study area (Figure 9). These results support the histograms of TMI solutions in Figure 8, which shows two distinct magnetic populations. Note that outliers (greater than two standard deviations) present in both data sets were removed prior to transformation to readily discriminate trends. The method of cumulative-frequency probability causes any normal distribution in a data set to be represented linearly (Morris Magnetics, personal communication, 1985). This is very beneficial with the current data sets, where a population with a higher frequency might shadow populations with a lower frequency. Additionally, the DC shift is quite prominent again. By applying simple lateral shifts of the observed magnetic susceptibility parallel to the x and y axes (Figure 9a) onto the apparent magnetic-susceptibility values, one can see they are almost identical in trend and shape (Figure 9b). The small local difference between the computed apparent susceptibility and the observed susceptibility values suggests minor errors exist in the acquisition of the observed TMI values. Although the much larger difference in content between

the two populations indicates that the surface susceptibility measurements were more predominant on altered granite surfaces.

Original highly detailed drill-core studies conducted on many borehole samples (Dugal et al., 1981; Morris, 1985; Lapointe et al., 1986; Harding et al., 1988) in the Eye-Dashwa Lakes pluton region showed three magnetic-susceptibility populations. This study has detected only two populations; however, this disagreement can be explained by having high alteration-zone geologic features present at depth that are not present at the surface. Bearing this in mind, the results show that two geophysical survey methods designed to measure different physical properties and at different scales can allow us to deduce one property from the other.

According to previous studies (Brown et al., 1980; Brown et al., 1984), the large lake in the study area is dominated by two northwest lineaments and the small lake is dominated by two northeast lineaments, which follow two of the three major linears within the pluton. In a geologic context, the TMI data exhibits both of these northeast and northwest fabrics, which is also observed in topographic data (Figure 1c) and aerial photos (Figure 1a). Without any additional information, it is unclear if these lineaments represent genuine fracture systems or are the result of a preferred sense of glacial scouring. In contrast, the apparent susceptibility data (Figure 7a) derived from the ground TMI survey defines a predominant northwest fabric. Verification of the validity of this fabric is provided by a limited number of in situ susceptibility readings (Figure 7b) over the same area that was covered by the TMI survey, and by detailed susceptibility log-

Figure 6. Cross section along profile 4400 (as in Figure 2) of the forward model designed to delineate magnetic-susceptibility variations on a local scale. Model incorporates a series of subvertical slabs that mimic altered fracture systems. Magnetic susceptibility of each slab has been indicated ($\times 10^{-2}$ SI).



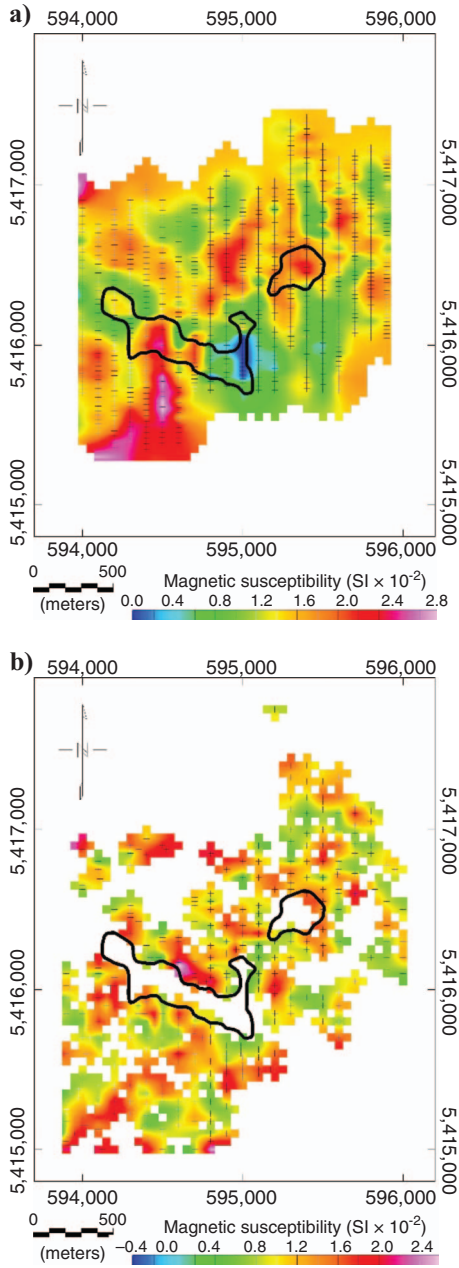


Figure 7. Grid comparison of (a) apparent and (b) observed magnetic susceptibilities. Both data sets have been gridded using a minimum-curvature interpolation. The grids are displayed with identical-color table ranges (2.8×10^{-2} SI), however they have a different point of origin that is consistent with a magnetic-susceptibility difference (DC shift) of 0.8×10^{-2} SI. Observation points are indicated with + signs.

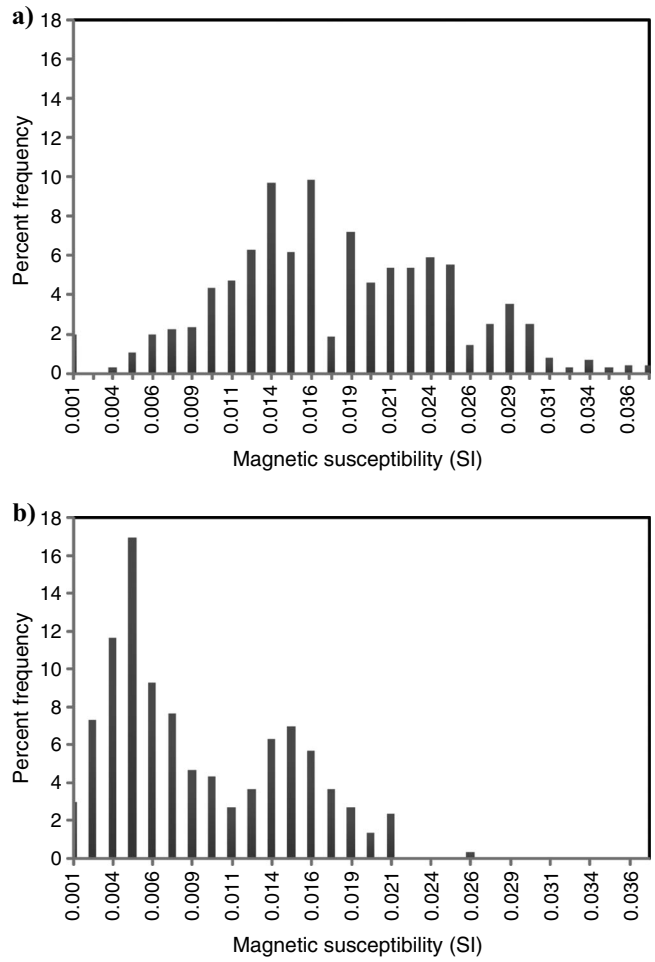


Figure 8. Comparison of magnetic-susceptibility data plotted versus percent frequency for (a) apparent and (b) observed magnetic susceptibilities. Both the apparent and observed magnetic-susceptibility data sets display a bimodal distribution.

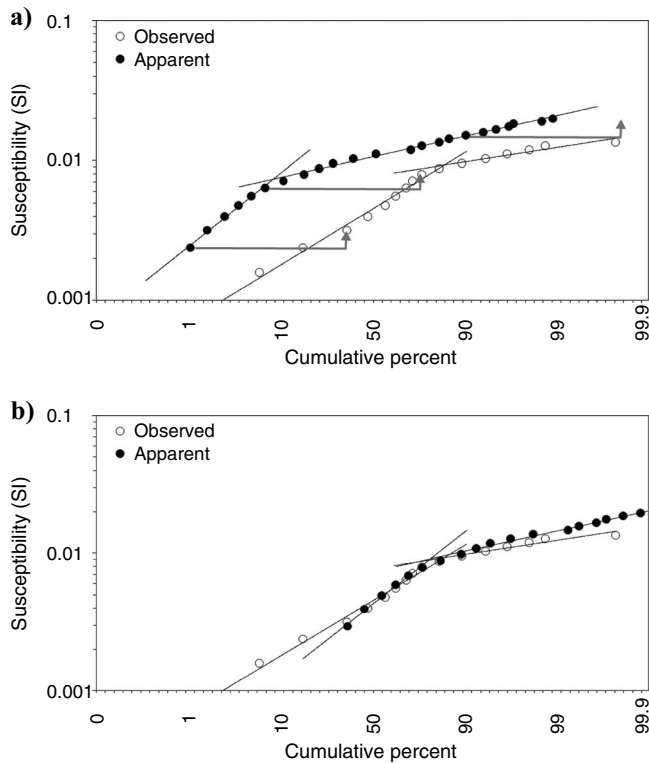


Figure 9. (a) Comparison of magnetic-susceptibility data plotted on a log scale versus its cumulative frequency plotted on a probability scale for observed and apparent magnetic susceptibilities. Two distinct populations of magnetic-susceptibility values can be identified, where each linear segment will represent the limitations of each population. (b) By applying a translation (indicated by arrows in [a]) to the apparent magnetic susceptibility, it is shown that the data sets are very similar in trend.

ging of a number of drill cores, which exhibited a diagnostic association between fractures and magnetic-susceptibility fluctuations.

CONCLUSIONS

This study demonstrates that in situations of limited accessibility, physical rock properties may be derived from geophysical methods. More specifically, it is shown that TMI data contains multiple levels of information that can be extracted if properly processed and interpreted, including apparent magnetic susceptibility and bathymetry estimates.

In the case of the Eye-Dashwa Lakes pluton, faults and fractures are mapped through reliable apparent magnetic-susceptibility values obtained from a high-resolution TMI data set. This method is useful in delineating surficial magnetic-susceptibility distribution but only when some structural information is provided. Based on previous studies, we knew that all faults and fracturing occurred sub-perpendicular to the ground surface dipping north. This knowledge was incorporated into all forward models. However, without this priori knowledge, a confident assessment on fracture distribution could not have been achieved because of the infinite-solution problem associated with potential field interpretation. Validation of the apparent susceptibility results were provided by an extensive set of mag-

netic-susceptibility measurements, which had been previously measured on core. Therefore, to use the method effectively and accurately, all available geoscientific data must be incorporated into the model.

Because of the strong magnetic contrast associated with the contact between water and ground, a TMI survey will inherently record information about the lake-bottom surface. This relationship permitted the calculation of two differently derived bathymetric data sets located in the Eye-Dashwa Lakes pluton. As a follow-up, it would be of interest to conduct an actual bathymetry survey to compare these depth results with the true values. This would allow us to verify whether this alternative method to depth estimation works. Furthermore, should the method prove valid, this could be applicable to remote locations that have limited to no ground exploration. This is especially true in Canada's northern regions, where a large portion of the land is covered with water bodies. Taking this approach one step further confirms that when looking at low-amplitude magnetic anomalies, all possible sources of magnetic signal contribution should be examined thoroughly.

REFERENCES

- Brown, P. A., D. Kamineni, D. Stone, and R. H. Thivierge, 1980, General geology of the Eye-Dashwa Lakes pluton, Atikokan, Northwestern Ontario: Atomic Energy of Canada Limited, Technical Record TR-108, <http://www.aecl.ca/newsroom/reports/library.htm>, accessed 07 April 2010.
- Brown, P. A., D. Stone, and N. Rey, 1984, Criteria from selecting new areas for geological investigation within the Eye-Dashwa Lakes pluton: Atomic Energy of Canada Limited, Technical Record TR-237, <http://www.aecl.ca/newsroom/reports/library.htm>, accessed 07 April 2010.
- Dugal, J. J. B., E. M. Hillary, D. C. Kamineni, and R. I. Sikorsky, 1981, Drilling and core logging programs at the Atikokan research area: Atomic Energy of Canada Limited, Technical Record TR-174, <http://www.aecl.ca/newsroom/reports/library.htm>, accessed 07 April 2010.
- Harding, K. A., W. A. Morris, S. J. Balch, P. Lapointe, and A. G. Latham, 1988, A comparison of magnetic character and alteration in the three granitic drill cores from Eastern Canada: *Canadian Journal of Earth Sciences*, **25**, 1141–1150.
- Hillary, E. M., 1982, Geometric representation of subsurface fracturing in boreholes ATK-1, ATK-2, ATK-3, ATK-4 and ATK-5, Atikokan, Northwestern Ontario (RA 4): Atomic Energy of Canada Limited, Technical Record TR-182, <http://www.aecl.ca/newsroom/reports/library.htm>, accessed 07 April 2010.
- Hillary, E. M., J. H. McEwen, and N. A. C. Rey, 1985, The evaluation of fracture zones at the Atikokan drill site and their geophysical response: Atomic Energy of Canada Limited, Technical Record TR-299, <http://www.aecl.ca/newsroom/reports/library.htm>, accessed 07 April 2010.
- Kamineni, D., and J. Dugal, 1981, A preliminary report and interpretation of alteration in the Eye-Dashwa Lakes pluton: Atomic Energy of Canada Limited, Technical Record TR-178, <http://www.aecl.ca/newsroom/reports/library.htm>, accessed 07 April 2010.
- , 1982, A study of rock lateration in the Eye-Dashwa Lakes pluton, Atikokan, Northwestern Ontario, Canada: *Chemical Geology*, **36**, 35–37.
- Kamineni, D., and D. Stone, 1983, The ages of fractures in the Eye-Dashwa Pluton, Atikokan, Canada: *Contributions to Mineralogy and Petrology*, **83**, 237–246.
- Lapointe, P., W. A. Morris, and K. L. Harding, 1986, Interpretation of magnetic susceptibility: A new approach to geophysical evaluation of the degree of rock alteration: *Canadian Journal of Earth Sciences*, **23**, 393–401.
- Morris Magnetics, personal communication, 1985.
- Pilkington, M., and J. B. Thurston, 2001, Draping corrections for aeromagnetic data: Line versus grid-based approaches: *Exploration Geophysics*, **32**, 95–101.
- Stone, D., 1980, Distribution of near-vertical surface fractures in the Dashwa pluton, Atikokan, Ontario: Atomic Energy of Canada Limited, Technical Record TR-299, <http://www.aecl.ca/newsroom/reports/library.htm>, accessed 07 April 2010.
- Stone, D., and D. Kamineni, 1982, Fractures and fracture infillings of the Eye-Dashwa Lakes pluton, Atikokan, Ontario: *Canadian Journal of Earth Sciences*, **19**, 789–803.